Coordination chemistry of lipoic acid and related compounds. Part 4.† Experimental and theoretical studies on the 1 : 2 proton complex of *N*-(1-adamantyl)lipoamide‡

Michaela Wilhelm, Rainer Koch* and Henry Strasdeit*

Fachbereich Chemie, Universität Oldenburg, Carl-von-Ossietzky-Str. 9–11, D-26129 Oldenburg, Germany. E-mail: henry.strasdeit@uni-oldenburg.de, rainer.koch@uni-oldenburg.de

N-(1-Adamantyl)lipoamide (**2**) has been prepared from racemic lipoic acid and reacted with hydrogen chloride in chloroform to afford [H(**2**)$_2$]Cl·xCHCl$_3$ (**3**). ^{1}H and ^{13}C NMR spectra of **3** in CDCl$_3$ show that **2** is protonated at the carbonyl oxygen atom. There are no indications of protonation at the amide N atom or the 1,2-dithiolane S atoms. X-Ray crystal structure analysis of **3** revealed the presence of the O-protonated dimer [H(**2**)$_2$]$^+$. The central part of this proton complex consists of a C=O···H$^+$···O=C hydrogen bridge with a short O···O distance of 2.439(4) Å. The C=O bonds [1.273(5) and 1.282(5) Å] are significantly lengthened and the (O)C–N bonds [1.313(5) and 1.311(5) Å] are shortened compared to the typical bond lengths in non-protonated secondary amides. The chloride ions interconnect the [H(**2**)$_2$]$^+$ complexes into infinite chains *via* N–H···Cl$^-$···H–N bridges [N···Cl 3.222(3) and 3.229(3) Å] and bind the solvent molecules *via* Cl$_3$CH···Cl$^-$ hydrogen bonds [C···Cl 3.361(6) and 3.386(7) Å]. Theoretical DFT and MP2 investigations on the model complex [H(**4**)$_2$]$^+$, where **4** is *N*-methylacetamide, indicate that the central proton is highly dynamic. It can almost freely shift within a ±0.1 Å range around the center of the O···O separation.

Lipoic acid, 5-(1,2-dithiolan-3-yl)pentanoic acid (**1**, see Scheme 1), acts as a coenzyme in biological group transfer reactions.[1–4] The bifunctionality of this molecule is vital to the role it plays in enzymes. While the carbonyl group is covalently attached to the peptide *via* an amide linkage involving the N$_\varepsilon$ atom of a lysine residue, the sulfur group shuttles between the disulfide, the dithiol and the acyl- or aminomethyl-group transferring state of the catalytic cycle.[5] Lipoic acid dependent enzymes are strongly inhibited by low micromolar concentrations of certain heavy metals and semimetals, for example Cd(II)[6] and As(III).[7] This inhibition is believed to be caused by the formation of 1,3-dithiolate chelate complexes from the dithiol (dihydrolipoyl) form.

Owing to its unique properties, **1** is of interest in metal coordination chemistry as a heteroditopic ligand and a building block for ligand syntheses. Until a few years ago, however, there were only scattered reports dealing with the preparation of coordination compounds of lipoic and dihydrolipoic acid.[8–15] Comprehensive solution studies on the interaction of **1** with biologically important metal ions were performed by Sigel and coworkers.[16] In recent years a number of new metal compounds of **1** and derivatives thereof have been isolated and structurally characterized. These include disulfide complexes of CuCl,[17] CuI, PdCl$_2$ and PdBr$_2$,[18] carboxylate complexes of Zn(II)[17,19] and Cd(II),[19] and thiolate complexes of As(III),[20] Cd(II)[21] and Hg(II).[22]

Like metal ions, the proton should also be capable of forming complexes with suitable derivatives of **1**. In fact, it has been proposed that the disulfide group of the enzymatic lipoyl-lysyl side chain becomes protonated, and thereby activated, before the group-transferring state is formed by reductive S–S

bond cleavage.[23] Although organic disulfides are only very weak bases, this hypothesis was reported to be consistent with the catalytic turnover numbers observed for the enzymes.

In the course of our investigations on new ligands derived from lipoic acid, we prepared *N*-(1-adamantyl)lipoamide (**2**, see Scheme 1). We noticed that **2** formed the crystalline proton complex [H(**2**)$_2$]$^+$ whose synthesis, spectroscopic properties and X-ray crystal structure are reported in the present paper. In addition, the results of theoretical calculations on a model complex are presented.
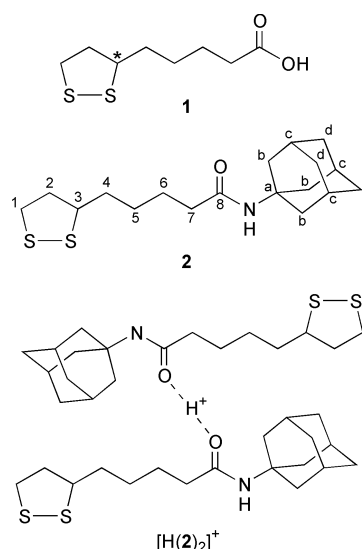
Scheme 1 Structures of lipoic acid **1**, the 1-adamantyl amide **2** and the proton complex [H(**2**)$_2$]$^+$. The atom labelling used with the NMR data is shown.

---

† For Part 3, see ref. 22.
‡ Dedicated to Professor Peter Köll on the occasion of his 60th birthday.

DOI: 10.1039/b107666c

Results and discussion

Syntheses and spectroscopic properties

N-(1-Adamantyl)lipoamide (**2**) is readily accessible *via* the imidazolide method (Scheme 2).[24] In order to obtain a satisfactory yield, a substantial excess of 1-adamantylamine should be employed. Column separation of **2** from the imidazolide of lipoic acid has been found difficult. Unreacted imidazolide was therefore transformed into ethyl lipoate by treatment with ethanol. **2** is a light-yellow crystalline substance.

A protonated form of **2** is obtained as [H(**2**)$_2$]Cl·xCHCl$_3$ (**3**) from solutions of **2** and hydrogen chloride in chloroform. Under favourable conditions, slow evaporation of such a solution gives crystals of **3** in which $x = 2$. A more reliable and reproducible route to **3** starts from a saturated HCl solution in CHCl$_3$ that contains approximately equimolar amounts of **2** and HCl. After removal of the solvent, the initially remaining oil solidifies within one week. The light-yellow solid still contains an excess of HCl, which is carefully removed by applying vacuum. By this method samples of **3** with a chloroform content of $x = 0.3$ are obtained. Attempts to remove the residual chloroform resulted in a complete loss of HCl, leaving **2**. Thus prolonged application of vacuum must be avoided.

Comparison of the ^{1}H and ^{13}C NMR spectra of **2** and **3** is particularly informative. The relevant data for solutions in CDCl$_3$ with an overall concentration of the amide of 50 mM are given in the Experimental section. In the ^{1}H NMR spectrum of **3**, the protons in the vicinity of the carbonyl group experience pronounced downfield shifts compared to **2** (NH: +2.64, H$_7$: +0.46, H$_b$: +0.09 ppm). In contrast, the resonances of the protons of the dithiolane ring (H$_1$ to H$_3$) remain unchanged within ±0.01 ppm. A similar picture is seen for the ^{13}C NMR spectrum. Strong shifts are observed for C$_7$, C$_8$ and C$_a$ (−2.01, +3.85 and +2.81 ppm, respectively). Again the atoms of the dithiolane ring are almost unaffected by the presence of hydrogen chloride (C$_1$: +0.07, C$_2$: +0.03, C$_3$: −0.16 ppm). These data clearly demonstrate that in solution the O or N atom is the main site of protonation.

There is no evidence for significant protonation at the disulfide group. This is also shown by a lack of concentration dependence of the resonances of the dithiolane ring atoms. In NMR spectra of **3**, recorded in the concentration range of 6–150 mM in CDCl$_3$, the maximum changes observed for H$_1$–H$_3$ and C$_1$–C$_3$ are only 0.02 and 0.23 ppm, respectively. The signals of the atoms in or near the amide group, however, experience considerable shifts on going from the lowest to the highest concentration studied (NH: +1.74, H$_7$: +0.20, C$_7$: −1.23, C$_8$: +1.53, C$_a$: +0.83 ppm). The H$^+$ signal moves from 9.2 to 12.2 ppm. The existence of concentration dependent shifts probably indicates an equilibrium between [H(**2**)$_2$]$^+$ and its dissociation products [H(**2**)]$^+$ and **2**.[25] But the interpretation of the data is not straightforward because other concentration dependent processes may also be involved, for example the formation of N–H···Cl$^-$ hydrogen bonds.
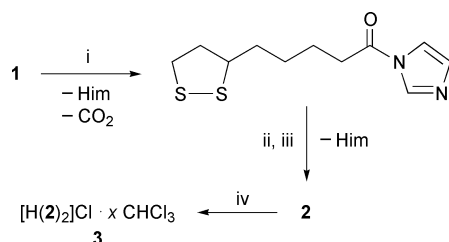
Mikhailov *et al.* reported that the signal of the acidic proton of [HA$_2$]$^+$ in chloroform is at 17.1 and 15.8 ppm for A = *N*-methylacetamide and *N,N*-diethylacetamide, respectively.[26] They used a saturated solution of the bromide and a 30% solution of the tribromide, respectively. The latter corresponds to a *ca.* 1.0–1.3 M solution. Such high concentrations are inaccessible for **3**. The lower value of 12.2 ppm measured for **3** may therefore be attributed to the considerably lower concentration of 0.15 M. It is also conceivable that, to a certain extent, unfavourable mutual orientations of the bulky substituents may hamper the association of [H(**2**)]$^+$ and **2** in solution.

The ^{1}H NMR spectrum of **3** allows a more precise localization of the protonation site within the amide group. There is strong evidence for O-protonation, which comes from three observations: (i) The half-width of the NH signal of **3** (*ca.* 22 Hz) is only twice as large as in the case of **2** (*ca.* 10 Hz). Seemingly no comparative values for N-protonated secondary amides are available, but it might be expected that proton exchange would give rise to a stronger line broadening if NH$_2$$^+$ groups were present. The observed moderate line broadening can be explained, for example, by N–H···Cl$^-$ interactions similar to those found in the solid state (see below). (ii) In the spectrum of **3**, an additional very broad signal occurs downfield (at 12.2 ppm, see above) from the NH signal. It appears unlikely that it belongs to NH$_2$$^+$ groups because proton exchange with the NH groups should be fast enough to result in a single resonance. Therefore, the signal is very probably due to C=O···H$^+$(···O=C) groups. (iii) The integral intensity of the NH signal of **3** exactly corresponds to two protons *per* two amide molecules. From the intensity of the signal at 12.2 ppm one acidic proton *per* two amides is calculated. In carboxylic amides, O-protonation is generally preferred to N-protonation.[27] Obviously compound **3** is no exception. This is further supported by a crystal structure determination.

Crystal structure of 3

In crystals of [H(**2**)$_2$]Cl·2CHCl$_3$ (**3**), the asymmetric unit comprises one formula unit whose amide molecules form a proton-bridged dimer (Fig. 1). Each [H(**2**)$_2$]$^+$ dimer is connected to two neighbouring dimers *via* N–H···Cl$^-$···H–N bridges. The resulting chain structure is shown in Fig. 2. The chloride ions are additionally involved in C–H···Cl$^-$ hydrogen bonds with the solvent molecules. The overall quality of the structure determination is slightly below average compared to those of other small-molecule structures. This is revealed, *inter alia*, by a conventional *R* value of 0.0730. The cause is, at least partly, that the dithiolane rings and the solvent molecules are disordered (see Experimental section).
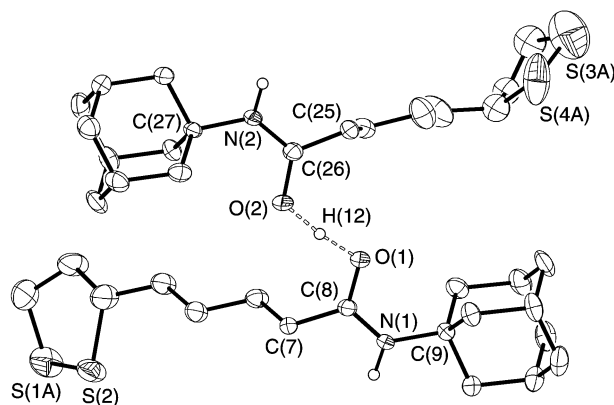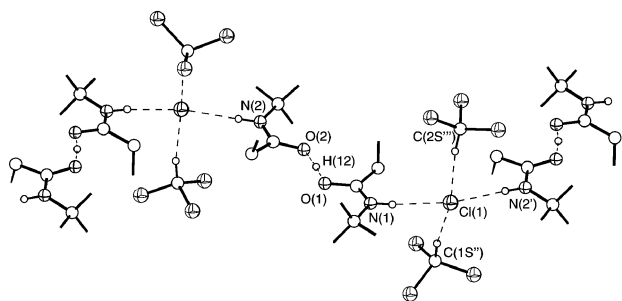

Scheme 2 *Reagents and conditions:* (i) *N,N′*-carbonyldiimidazole, THF, r.t., 8 h; (ii) 1-adamantylamine, reflux, 48 h; (iii) EtOH, reflux, 2–4 h; (iv) HCl in chloroform, r.t., 1 h. Him = imidazole.

Fig. 1 Structure of the proton complex [H(**2**)$_2$]$^+$ in crystals of [H(**2**)$_2$]Cl·2CHCl$_3$ (**3**). Displacement ellipsoids are drawn at the 30% probability level. Carbon-bonded H atoms have been omitted.

Fig. 2 The chain structure that is formed by alternately arranged [H(**2**)$_2$]$^+$ cations and weakly chloroform-coordinated chloride ions in crystals of [H(**2**)$_2$]Cl·2CHCl$_3$ (**3**). For the sake of clarity, only the central parts of the amide molecules are shown. H atoms not involved in hydrogen bonds (broken lines) are omitted. Atom sizes are arbitrary.

Scheme 3

Fortunately, the more interesting parts of the structure, namely the amide groups and their vicinity, are well-ordered. Relevant interatomic distances and angles are given in Table 1.

The most striking feature of the crystal structure of **3** is the short distance of 2.439(4) Å between the carbonyl oxygen atoms O(1) and O(2), which is 0.64 Å smaller than the van der Waals distance.[28] The Cambridge Structural Database (V. 5.21, April 2001 release)[29] currently contains 44 entries where the distance between two carboxylic amide O-atoms is ≤2.60 Å. The result subdivides into three groups of compounds: (i) hemiprotonated carboxylic amides arranged into dimers with C=O···H$^+$···O=C bridges (16 compounds); (ii) metal and metalloid complexes with O-coordinated carboxylic amide ligands; here short O···O contacts in the first coordination sphere are forced by the coordination geometries, the coordination numbers and/or small central atoms; (iii) metal complexes with short C=O···O=C distances in higher coordination spheres; these cases are restricted to complexes of the purpurato ligand.[30]

From structural similarities to compounds belonging to group (i) it can be concluded that in **3** a C=O···H$^+$···O=C bridge is present too. Further evidence comes from comparison with the typical bond lengths in the N–C=O fragment of non-protonated secondary amides. Boks determined average C=O and C–N bond lengths of 1.230 and 1.331 Å, respectively.[31] Compared to these values the C=O bonds in **3** are
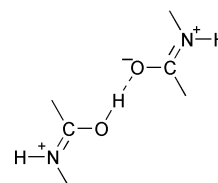
lengthened by 0.043 and 0.052 Å, while the corresponding C–N bonds are 0.018 and 0.020 Å shorter. These changes are compatible with O-protonation and strong participation of resonance forms such as the one shown in Scheme 3, but not with N-protonation.

The fact that the C=O bond lengths in **3** differ by only 0.009 Å or two estimated standard deviations indicates either a symmetric position or a statistical disorder of the proton between the O atoms. This situation is encountered in most of the hemiprotonated carboxylic amides of group (i). However, one exception is worth mentioning, namely the [H(phenacetin)$_2$]$^+$ dimer.[32] There, despite the presence of a short O···O contact [2.432(4) Å], the C=O bond lengths are significantly different [1.283(6) and 1.245(6) Å], indicating asymmetric hydrogen bonding.

Each chloride ion of **3** is involved in four hydrogen bonding interactions. Two N–H···Cl$^-$ and two Cl$_3$C–H···Cl$^-$ hydrogen bonds occur with corresponding N···Cl and C···Cl distances of 3.222(3), 3.229(3) Å and 3.361(6), 3.386(7) Å, respectively. These data compare with the mean values recently given by Steiner for >Nsp^2–H···Cl$^-$ (3.181 Å) and Cl$_3$C–H···Cl$^-$ (3.42 Å) hydrogen bonds.[33] N–H···Cl$^-$···H–N bridges connecting [H(amide)$_2$]$^+$ dimers into infinite chains were also found in the hemihydrochloride of N-methylacetamide (**4**), [H(**4**)$_2$]Cl.[34] This compound bears some further close similarities to **3**; for example, the O···O distance of 2.429(3) Å [**3**: 2.439(4) Å] and the C=O bond length of 1.268(3) Å [**3**: 1.273(5) and 1.282(5) Å]. In both compounds, the five-atom moieties CC(=O)NC are essentially planar, the maximum deviations from the least-squares planes being 0.021 Å [N(1)] and 0.057 Å [N(2)] for **3** and 0.006 Å (N) for [H(**4**)$_2$]Cl. The cations [H(**2**)$_2$]$^+$ and [H(**4**)$_2$]$^+$ can formally be regarded as homoleptic proton complexes similar to alkali metal amide complexes such as [Li(**4**)$_4$]$^+$.[35] There are, however, characteristic geometric and energetic differences between hydrogen bonds and, for example, lithium bonds.[36] From a methodological view, a major difference concerns the way in which the position of the central atom can be determined: in contrast to a metal ion, the proton cannot be localized directly from X-ray diffraction data.

Quantum-mechanical results

From the above discussion of the crystal structure of **3** it is obvious that the exact position of the hydrogen atom located between the two oxygen atoms is unknown. We therefore decided to apply quantum-mechanical methods in order to gain more insight into the structural and energetic details of very short O···H$^+$···O hydrogen bonds between carboxylic amide molecules. As a model we used N-methylacetamide (**4**), well-known as the subject of various theoretical studies,[27a,37] which is computationally less demanding than **2**. Furthermore, there exists several computational investigations of proton transfer processes,[38] including O···H···O hydrogen bonding,[39] and a literature-based analysis of O···H···O containing structures determined from neutron diffraction data.[40] From the latter it can be concluded that an O···O distance of 2.44 Å, as found in **3**, should correspond to a structure with two different O–H bonds, being around 1.09 and 1.35 Å.

Table 1 Selected interatomic distances (in Å), bond angles and torsion angles (in degrees) for [H(**2**)$_2$]Cl·2CHCl$_3$ (**3**)^a

C(8)–O(1)	1.273(5)	C(26)–O(2)	1.282(5)
C(8)–N(1)	1.313(5)	C(26)–N(2)	1.311(5)
C(9)–N(1)	1.490(5)	C(27)–N(2)	1.488(5)
C(7)–C(8)	1.501(5)	C(25)–C(26)	1.492(6)
S(1A)–S(2)	2.012(3)	O(1)···O(2)	2.439(4)
Cl(1)···N(1)	3.222(3)	Cl(1)···N(2')	3.229(3)
Cl(1)···C(1S'')	3.361(6)	Cl(1)···C(2S''')	3.386(7)
C(8)–O(1)···O(2)	115.0(3)	C(26)–O(2)···O(1)	116.3(3)
C(8)–N(1)–C(9)	127.6(3)	C(26)–N(2)–C(27)	127.5(3)
O(1)–C(8)–N(1)	120.6(4)	O(2)–C(26)–N(2)	120.1(4)
O(1)–C(8)–C(7)	120.8(4)	O(2)–C(26)–C(25)	120.6(4)
N(1)–C(8)–C(7)	118.6(3)	N(2)–C(26)–C(25)	119.2(4)
C(9)–N(1)–C(8)–O(1)	−1.5(7)	C(27)–N(2)–C(26)–O(2)	−5.1(7)
C(9)–N(1)–C(8)–C(7)	176.6(4)	C(27)–N(2)–C(26)–C(25)	171.5(4)
C(8)–O(1)···O(2)–C(26)	−168.4(4)		

^{a} Symmetry transformations used to generate equivalent atoms: $'$−x+1, y+0.5, −z+0.5; $''$ −x+1, −y+1, −z; $'''$ −x+1, −y+1, −z+1.

The proton complex $[H(4)_2]^+$ was optimized at the HF, B3LYP and MP2 levels of theory employing the 6-31++G(d,p) basis set, which includes diffuse functions at all atoms, thus improving the description of the relatively weak interactions between the hydrogen and oxygen atoms. Not surprisingly, the results differ quite significantly depending on the utilized method (Table 2): the calculations at the Hartree–Fock level give a structure with strong asymmetric hydrogen bonding (O–H: 1.002 and 1.503 Å) as the minimum, while a constrained symmetric geometry (two symmetric O–H distances: 1.181 Å, one imaginary frequency corresponding to the movement of the hydrogen atom between the two oxygen atoms) lies about 8 kJ mol^{-1} higher in energy. Taking into account the zero-point vibrational energy (ZPVE) correction, the symmetric structure becomes favourable by 3 kJ mol^{-1}. In contrast, all attempts to minimize a comparable asymmetric structure at the B3LYP/6-31++G(d,p) level failed; only a symmetric one is a stable minimum at this level with an O–H distance of 1.201 Å. The MP2 approach finds two structures, one with O–H contacts of 1.163 and 1.236 Å and one with the hydrogen atom placed exactly in the center between the two oxygen atoms. Both minima possess essentially the same energy, the difference being less than a hundredth of a kJ mol^{-1}, including ZPVE there was still less than one kJ mol^{-1} in favour of the symmetric geometry. The interconversion barrier is therefore very small, allowing the proton to move freely from one asymmetric isomer to its mirror image via the symmetric structure. However, the calculations cannot unequivocally determine the position of the proton. It appears to be located close to the center of the O···O separation, possibly being integrated into two O–H bonds of the same length.

A comparison of selected geometrical features of the calculated structures of $[H(4)_2]^+$ with experimental data from the X-ray structure analysis of 3 is given in Table 3. Additionally, some relevant bond lengths and angles from the crystal structure[34] of N-methylacetamide hemihydrochloride, $[H(4)_2]Cl$, are included.

Again, the Hartree–Fock-based calculations cannot accurately reproduce the experimental structures, the main failure being the much too long O···O contact. The calculations at the B3LYP and MP2 levels find (O)C–N bonds that are slightly too long and a central O···O distance that is 0.03–0.04 Å too short. The calculated angles agree well with those of the X-ray structures. It is worth mentioning that a mutual twisting of the two hydrogen-bonded amide molecules occurs in the experimental structure of $[H(4)_2]^+$ and, much less pronounced, in 3, in contrast to the calculated coplanar arrangement. We attribute this torsion to crystal packing effects that are unaccounted for by gas phase calculations.

The nonexistent energy difference between the two MP2-calculated geometries and the appearance of only one DFT-determined structure indicate a non-localized proton within a certain range of O–H distances. In order to further evaluate this movement, additional B3LYP/6-31++G(d,p) calculations were performed. We fixed one of the two O–H distances, while the rest of the molecule was allowed to relax. Starting from the symmetrical minimum, the frozen O–H bond length was both incremented and decreased in small (0.03 Å) steps. In Fig. 3, the two O–H lengths (one constrained, one free) are plotted against the O···O distance. Only the lengthening of the frozen O–H bond (together with the resulting O–H and O···O distances) is shown, as the plot for the shortening of this bond is very similar.
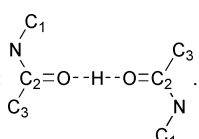
In excellent agreement with a plot derived from neutron diffraction data,[40] there exists a minimum for the O···O distance at 2.40 Å (neutron diffraction: ca. 2.39 Å),

Table 2 Calculated relative energies (in kJ mol^{-1}) and O–H bond lengths (in Å) of $[H(4)_2]^+$ (values in parentheses: energies without scaled ZPVE correction)

Structure		HF/ 6-31++G(d,p)	B3LYP/ 6-31++G(d,p)	MP2/ 6-31++G(d,p)
Asymmetric	O–H distance	1.002/1.505	—	1.163/1.236
	Relative energy	3.0 (−7.8)	—	0.7 (−0.004)
Symmetric	O–H distance	1.181	1.201	1.198
	Relative energy	0.0	0.0	0.0

Table 3 Comparison of calculated main geometrical parameters of $[H(4)_2]^+$ and data from crystal structures of 3 and $[H(4)_2]Cl$. Distances are in Å and angles in degrees[a]

	HF asymmetric	B3LYP symmetric	MP2 asymmetric	MP2 symmetric	3 X-ray	$[H(4)_2]Cl$ X-ray
C2–O	1.269/1.233	1.274	1.283/1.277	1.280	1.282/1.273	1.268
C2–C3	1.495/1.505	1.503	1.497/1.499	1.498	1.492/1.501	1.489
C1–N	1.467/1.456	1.467	1.465/1.463	1.464	1.488/1.490	1.452
C2–N	1.296/1.320	1.325	1.321/1.325	1.323	1.311/1.313	1.305
O···O	2.505	2.402	2.399	2.396	2.439	2.429
O–H	1.002/1.503	1.201	1.163/1.236	1.198	(1.22)	
O–C2–N	117.6/120.8	118.6	118.1/118.6	118.3	120.1/120.6	119.3
O–C2–C3	121.0/121.0	121.8	121.7/121.6	121.6	120.6/120.8	121.7
N–C2–C3	121.3/118.3	119.6	120.3/119.8	120.0	119.2/118.6	119.0
C1–N–C2	124.1/123.1	123.6	122.7/122.6	122.6	127.5/127.6	123.5
C2–O···O	113.4/134.1	119.2	115.0/117.6	116.2	115.0/116.3	120.1
Angle between mean planes[b]	0	0	0	0	12.5	62.4

[a] Numbering scheme:

$$\begin{array}{c} C_1 \\ | \\ N \qquad\qquad C_3 \\ \diagdown \qquad \diagup \\ C_2{=}O{-}\!-H{-}\!-O{=}C_2 \\ \diagup \qquad \diagdown \\ C_3 \qquad\qquad N \\ | \\ C_1 \end{array}$$

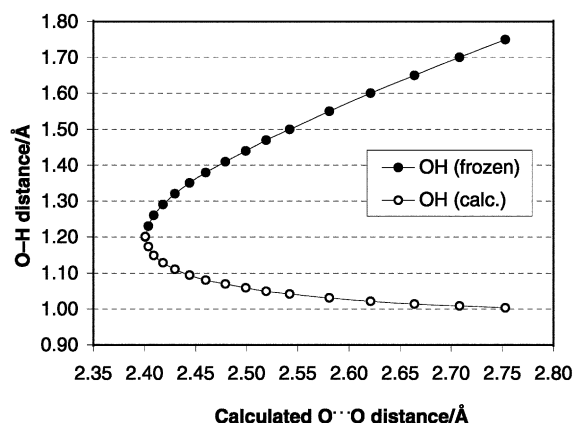. [b] Mean planes are defined by the two sets of atoms O, N, C1, C2 and C3.

Fig. 3 B3LYP/6-31++G(d,p)-calculated O–H and O···O distances in $[H(4)_2]^+$ with one restrained O–H bond.

corresponding to symmetric O···H···O hydrogen bonds. Also, the shapes of the two curves are almost identical, indicating the very good description of the herein studied hydrogen bonds by the employed DFT method. Applying the O···O distance of 2.44 Å experimentally found for **3**, the corresponding O–H bond lengths can be determined from Fig. 3 as 1.10 and 1.34 Å, hence indicating a slight asymmetry of the hydrogen bond.

The energetic consequences of the O–H variation are shown in Fig. 4 where the relative energy of the system as a function of the constrained O–H bond is given. One can clearly identify a potential well that ranges from O–H distances of 1.09 to 1.35 Å, for which the energy difference with respect to the symmetric minimum is less than 0.5 kJ mol^{-1}. This further indicates that the proton is allowed to travel almost freely, at least within this region. Calculation of a structure with a fixed O···O contact of 2.44 Å, corresponding to the X-ray structure of **3**, lies only 0.38 kJ mol^{-1} higher in energy than the symmetric minimum with an O···O distance of 2.40 Å. The resulting O–H bond lengths of 1.119 and 1.321 Å are in accordance with the above found values derived from Fig. 3.

From a theoretical point of view, these calculations suggest the occurrence of symmetrical hydrogen bonds, although the mobility of the proton in the gas phase indicates that the investigated system is highly dynamic. The very small energy differences between asymmetric and symmetric structures at both the DFT and MP2 levels of theory, prohibit more exact inferences concerning the position of the proton in the crystal structure of **3**. Both the O···O distance and the nature of the hydrogen bonds are governed by factors such as the dipolar environment, intermolecular hydrogen bonds (*e.g.*, N–H···Cl$^-$, see above) and crystal packing. It should be kept in mind, that, of course, that the calculations ignore these forces altogether, and hence the excellent overall agreement observed is very remarkable indeed.

Experimental

Materials and instruments

1-Adamantylamine was prepared by treating the commercially available 1-adamantylamine hydrochloride with a slight excess of triethylamine in dichloromethane, followed by washing the solution with water and removing the dichloromethane under reduced pressure. Tetrahydrofuran was refluxed over sodium for 4 h and then distilled to remove the stabilizer, 2,6-di(*tert*-butyl)-4-methylphenol. Other solvents were dried with 3 Å molecular sieves. Prior to use in the NMR experiments, CDCl$_3$ was treated with silver oxide[41] and 3 Å molecular sieves for some hours to remove traces of hydrogen chloride and water. Hydrogen chloride gas was generated by dropping concentrated H$_2$SO$_4$ into sodium chloride and passed through concentrated H$_2$SO$_4$ before it was used to prepare a saturated solution in chloroform. The other starting materials, including racemic lipoic acid ($\geq$98%), were purchased from commercial sources and used without further purification.

^{1}H (300.13 MHz) and ^{13}C{^{1}H} (75.47 MHz) NMR spectra were recorded with a Bruker AM 300 spectrometer at room temperature. Chemical shifts are given relative to SiMe$_4$ ($\delta = 0.00$). In ^{13}C NMR spectra the solvent signal was used as internal reference (CDCl$_3$: $\delta_C = 77.00$). Signal assignments were made from 2D NMR spectra and by comparison with published spectra[42] of **1** and lipoamide. Infrared spectra were obtained on an FT-IR spectrometer Bio-Rad FTS 7PC. Mass spectra were measured with a Finnigan MAT 212 instrument. Elemental analyses were performed by the Microanalytical Laboratory Pascher (Remagen-Bandorf, Germany) and the Analytical Laboratories Malissa and Reuter (Lindlar, Germany).

Syntheses

N-(1-Adamantyl)lipoamide (2). *N,N'*-Carbonyldiimidazole (3.24 g, 20.0 mmol) was added to a solution of *rac*-lipoic acid (4.13 g, 20.0 mmol) in dry tetrahydrofuran (50 ml). The reaction mixture was stirred at room temperature for 8 h. After addition of 1-adamantylamine (6.05 g, 40.0 mmol, 100% excess), the solution was refluxed for 48 h. If unreacted imidazolide of lipoic acid was still present afterwards (checked by TLC), ethanol (20 ml) was added, and the solution was again refluxed until the imidazolide was no longer detectable (2–4 h). Then most of the solvent was removed under reduced pressure. The remaining yellow suspension was subjected to a column separation [column length: 50 cm, diameter: 6 cm; silica gel 60, particle size: 0.063–0.200 mm (70–230 mesh ASTM); *n*-hexane–tetrahydrofuran 1 : 1. TLC with the same eluent on silica gel gave $R_f \approx 0.75$ for **2**]. **2** was contained in the second band. It was obtained as small light-yellow crystal needles after evaporation of the solvent *in vacuo*. Yield: 4.8 g (71%). M.p. 83 °C. Anal. calcd for C$_{18}$H$_{29}$NOS$_2$: C, 63.67; H, 8.61; N, 4.12; S, 18.89; found: C, 63.60; H, 8.59; N, 4.09; S, 18.79%. IR (KBr, cm^{-1}): 3291s, 3061m, 2913vs, 2901vs, 2847s, 1636vs, 1547s, 1451m, 1360m, 1275m, 1229m, 1136m, 694m, 650m, 559m. ^{1}H NMR (0.05 M in CDCl$_3$): δ 1.45 (m, 2H, H$_5$), 1.67 (m, 10H, H$_4$/H$_6$/H$_d$), 1.90 (m, 1H, H$_2$), 1.99 (s, 6H, H$_b$), 2.08 (m, 5H, H$_7$/H$_c$), 2.45 (m, 1H, H$_{2'}$), 3.14 (m, 2H, H$_1$), 3.57 (m, 1H, H$_3$), 5.08 (br, s, 1H, NH). ^{13}C NMR (0.05 M in CDCl$_3$): δ 25.40 (C$_6$), 28.77 (C$_5$), 29.45 (C$_c$), 34.64 (C$_4$), 36.36 (C$_d$), 37.44 (C$_7$), 38.44 (C$_1$), 40.23 (C$_2$), 41.72 (C$_b$), 51.81 (C$_a$), 56.47 (C$_3$), 171.78 (C$_8$). CI-MS (isobutane): *m/z* 340 ([M + H]$^+$, 100%).

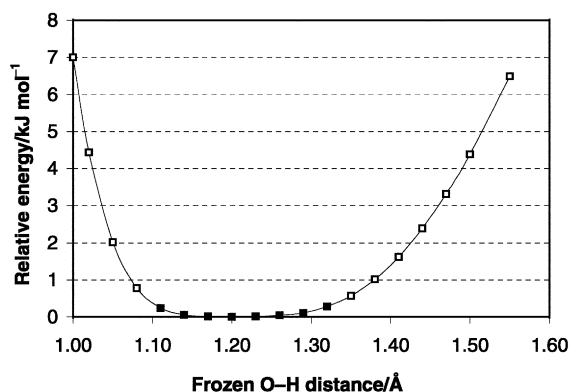**Fig. 4** Relative energies (in kJ mol^{-1}) of $[H(4)_2]^+$ with one restrained O–H bond (■ indicates a relative energy of less than 0.5 kJ mol^{-1}).

[H(2)$_2$]Cl·xCHCl$_3$ (3). 2 (0.68 g, 2.0 mmol) was dissolved in chloroform (8.0 ml) saturated with HCl (*ca.* 2.2 mmol). After 1 h the solvent and excess HCl were removed *in vacuo*. Within 7 days the remaining yellow oil transformed into a light-yellow microcrystalline solid, which was detached from the wall of the flask, but not further grinded. The solid was dried *in vacuo* (0.5 mbar) for 8 h. By this procedure a product was obtained for which x was 0.3 as judged by ^{1}H NMR (in CD$_2$Cl$_2$) and elemental analysis (see below). Yield: 0.72 g (96%). Anal. calcd for C$_{36.3}$H$_{59.3}$Cl$_{1.9}$N$_2$O$_2$S$_4$: C, 58.02; H, 7.95; Cl$_{total}$ 8.96; Cl$_{ionic}$ 4.72; N, 3.73; S, 17.07; found: C, 57.70; H, 8.09; Cl$_{total}$ 9.00; Cl$_{ionic}$ 5.05; N, 3.71; S, 16.9%. IR (KBr, cm^{-1}): *ca.* 3200wbr, *ca.* 3020wsh, 2907vs, 2851s, 1653m, 1543w, 1454m, 1360m, 1256w, 1005m, 970w, 918m, 814m, 746s, 648m, 552w. ^{1}H NMR (0.025 M in CDCl$_3$): δ 1.52 (m, 4H, H$_5$), 1.69 (m, 20H, H$_4$/H$_6$/H$_d$), 1.91 (m, 2H, H$_2$), 2.08 (m, 18H, H$_b$/H$_c$), 2.46 (m, 2H, H$_{2'}$), 2.54 (m, 4H, H$_7$), 3.13 (m, 4H, H$_1$), 3.58 (m, 2H, H$_3$), 7.72 (br, s, 2H, NH), 11.0 (vbr, s, 1H, O···H$^+$). ^{13}C NMR (0.025 M in CDCl$_3$): δ 26.26 (C$_6$), 28.51 (C$_5$), 29.32 (C$_c$), 34.45 (C$_4$), 35.43 (C$_7$), 36.07 (C$_d$), 38.51 (C$_1$), 40.26 (C$_2$), 41.04 (C$_b$), 54.62 (C$_a$), 56.31 (C$_3$), 175.63 (C$_8$). CI-MS (isobutane): m/z 679 ([H(2)$_2$]$^+$, 10%), 340 ([2 + H]$^+$, 100%).

X-Ray crystal structure analysis of 3 (x = 2)

A suitable single crystal was obtained by slow evaporation of a solution of **2** and HCl in chloroform. The light-yellow crystal was embedded in perfluoropolyalkylether [viscosity 1600 cSt., m.p. −20 °C; ABCR (Karlsruhe, Germany)] and placed into a glass capillary. The capillary was sealed and transferred into the cold gas stream of a STOE IPDS area detector diffractometer. Mo-Kα radiation (λ = 0.71073 Å) was used for intensity data collection. Crystal data and structure refinement: C$_{38}$H$_{61}$Cl$_7$N$_2$O$_2$S$_4$, M = 954.3, monoclinic, space group $P2_1/c$, a = 12.915(1), b = 19.757(1), c = 19.010(1) Å, β = 102.34(1)°, U = 4738.6(5) Å^3, Z = 4, D_c = 1.338 g cm^{-3}, μ(Mo-Kα) = 6.29 cm^{-1}, T = 193 K, reflections: 34 786 collected, 8750 independent (R_{int} = 0.0812), 4362 observed [$I > 2\sigma(I)$]; numerical absorption correction, refinement on F^2, R_1 = 0.0730 [$I > 2\sigma(I)$], wR_2 = 0.2259 (all data).

The structure was solved in space group $P1$ by direct methods. The initial structural model was then transferred into space group $P2_1/c$ and further refined. In the final model, the two dithiolane rings of the asymmetric unit are disordered to different degrees. In the first ring, only the sulfur atom S(1) had to be refined in two positions (occupancy ratio A : B = 0.85 : 0.15), while in the second one two equally occupied split positions were introduced for each of the atoms S(3), S(4), C(19), C(20) and C(21). In this second ring, the changes of some of the interatomic distances were restrained during the refinement (DFIX instructions). Each of the Cl atoms of the two independent solvent molecules was refined as disordered on two positions (molecule 1, A : B = 0.75 : 0.25) and three positions (molecule 2, A : B : C = 0.50 : 0.25 : 0.25), respectively. Anisotropic displacement parameters were refined for the non-hydrogen atoms, except S(1B), C(19A,B), C(20A,B) and C(21A,B). Hydrogen atoms were included in idealized positions. A hydrogen atom H(12) was arbitrarily positioned halfway between the carbonyl oxygen atoms O(1) and O(2) (DFIX instructions). This did not significantly change the O(1)···O(2) distance. Programs used were those of the SHELX-97 software package[43] and DIAMOND.[44]

CCDC reference number 181550. See http://www.rsc.org/suppdata/nj/b1/b107666c/ for crystallographic data in CIF or other electronic format.

Computational details

The structure of **4** was optimized at the Hartree–Fock, the hybrid functional Becke3LYP,[45] and the second-order Møller–Plesset[46] levels of theory with the 6-31++G(d,p) basis set, employing the program package Gaussian 98.[47] All obtained structures were verified as local minima or transition states through harmonic frequency calculations. Zero-point vibrational energies are scaled with the appropriate scaling factors for the different levels of theory.

References and notes

1 D. Voet and J. G. Voet, *Biochemistry*, Wiley, New York, 2nd edn., 1995, pp. 541ff and 736ff.
2 A. Berg and A. de Kok, *Biol. Chem.*, 1997, **378**, 617.
3 D. J. Oliver, *Annu. Rev. Plant Physiol. Plant Mol. Biol.*, 1994, **45**, 323.
4 *Alpha-Keto Acid Dehydrogenase Complexes*, eds. T. E. Roche and M. S. Patel, New York Academy of Sciences, New York, 1989.
5 For relevant X-ray crystallographic studies see: M. Faure, J. Bourguignon, M. Neuburger, D. Macherel, L. Sieker, R. Ober, R. Kahn, C. Cohen-Addad and R. Douce, *Eur. J. Biochem.*, 2000, **267**, 2890.
6 Z. Tynecka and A. Malm, *J. Basic Microbiol.*, 1996, **36**, 447.
7 Y. Hu, L. Su and E. T. Snow, *Mutat. Res. DNA Repair*, 1998, **408**, 203 and references therein.
8 F. Bonomi, S. Pagani, F. Cariati, A. Pozzi, G. Crisponi, F. Cristiani, V. Nurchi, U. Russo and R. Zanoni, *Inorg. Chim. Acta*, 1992, **195**, 109.
9 F. Bonomi, S. Pagani, F. Cariati, A. Pozzi, G. Crisponi, F. Cristiani, A. Diaz and R. Zanoni, *Inorg. Chim. Acta*, 1992, **192**, 237.
10 K. Dill, E. R. Adams, R. J. O'Connor and E. L. McGown, *Chem. Res. Toxicol.*, 1989, **2**, 181.
11 A. Shaver, O. Lopez and D. N. Harpp, *Inorg. Chim. Acta*, 1986, **119**, 13.
12 C. H. Banks, J. R. Daniel and R. A. Zingaro, *J. Med. Chem.*, 1979, **22**, 572.
13 P. R. Brown and J. O. Edwards, *J. Inorg. Nucl. Chem.*, 1970, **32**, 2671.
14 P. R. Brown and J. O. Edwards, *Biochemistry*, 1969, **8**, 1200.
15 M. Webb, *Biochim. Biophys. Acta*, 1962, **65**, 47.
16 H. Sigel, *Angew. Chem., Int. Ed. Engl.*, 1982, **21**, 389 and references therein.
17 M. R. Baumgartner, H. Schmalle and E. Dubler, *Inorg. Chim. Acta*, 1996, **252**, 319; A note on the Zn(II) carboxylate complex appeared earlier: E. Dubler, G. B. Jameson, N. Cathomas, M. Baumgartner and A. Reller, *Acta Crystallogr., Sect. A*, 1984, **40**, C-311.
18 A. von Döllen, Doctoral thesis, University of Oldenburg, Germany, 1997.
19 H. Strasdeit, A. von Döllen and A.-K. Duhme, *Z. Naturforsch., B*, 1997, **52**, 17.
20 A. von Döllen and H. Strasdeit, *Eur. J. Inorg. Chem.*, 1998, 61.
21 A.-K. Duhme, Doctoral thesis, University of Oldenburg, Germany, 1993.
22 H. Strasdeit, A. von Döllen, W. Saak and M. Wilhelm, *Angew. Chem., Int. Ed.*, 2000, **39**, 784.
23 K. Pan and F. Jordan, *Biochemistry*, 1998, **37**, 1357.
24 H. A. Staab, H. Bauer and K. M. Schneider, *Azolides in Organic Synthesis and Biochemistry*, Wiley-VCH, Weinheim, 1998, pp. 14–16 and 129–140.
25 A recent NMR study on a system that shows concentration dependent formation of H-bonded dimers and oligomers is presented in: M. Mascal, C. E. Marjo and A. J. Blake, *Chem. Commun.*, 2000, 1591.
26 V. A. Mikhailov, D. S. Yufit and Y. T. Struchkov, *J. Gen. Chem. USSR (Engl. Transl.)*, 1992, **62**, 322.
27 See, for example: (*a*) A. Bagno, B. Bujnicki, S. Bertrand, C. Comuzzi, F. Dorigo, P. Janvier and G. Scorrano, *Chem. Eur. J.*, 1999, **5**, 523; (*b*) S. J. Cho, C. Cui, J. Y. Lee, J. K. Park, S. B. Suh,

J. Park, B. H. Kim and K. S. Kim, *J. Org. Chem.*, 1997, **62**, 4068 and references in both.

28 S. C. Nyburg and C. H. Faerman, *Acta Crystallogr., Sect. B*, 1985, **41**, 274.

29 (*a*) F. H. Allen and O. Kennard, *Chem. Des. Autom. News*, 1993, **8**, 1; (*b*) F. H. Allen and O. Kennard, *Chem. Des. Autom. News*, 1993, **8**, 31.

30 See, for example: A. H. White and A. C. Willis, *J. Chem. Soc., Dalton Trans.*, 1977, 1377.

31 G. J. Boks, Doctoral thesis, University of Utrecht, The Netherlands, 1997; available under http://www.library.uu.nl/digiarchief/dip/diss/01741627/boks.html.

32 F. H. Herbstein, M. Kapon and W. Schwotzer, *Helv. Chim. Acta*, 1983, **66**, 35.

33 T. Steiner, *Acta Crystallogr., Sect. B*, 1998, **54**, 456.

34 M. Jaber, J. Guilhem and H. Loiseleur, *Acta Crystallogr., Sect. C*, 1983, **39**, 485; revision of the space group: R. E. Marsh, *Acta Crystallogr., Sect. C*, 1983, **39**, 1473.

35 P. Chakrabarti, K. Venkatesan and C. N. R. Rao, *Proc. R. Soc. London, Ser. A*, 1981, **375**, 127.

36 S. Scheiner, in *Lithium Chemistry: A Theoretical and Experimental Overview*, eds. A.-M. Sapse and P. v. R. Schleyer, Wiley, New York, 1995, p. 67.

37 H. Guo and M. Karplus, *J. Phys. Chem.*, 1992, **96**, 7273; N. G. Mirkin and S. Krimm, *J. Mol. Structure (THEOCHEM)*, 1995, **334**, 1; W. G. Han and S. Suhai, *J. Phys. Chem.*, 1996, **100**, 3942; I. N. Demetropoulos, I. P. Gerothanassis, C. Vakka and C. Kakavas, *J. Chem. Soc., Faraday Trans.*, 1996, **92**, 921.

38 See, for example: S. Scheiner and L. Wan, *J. Am. Chem. Soc.*, 1993, **115**, 1958; C. F. Rodriguez, A. Cunje, T. Shoeib, I. K. Chu, A. C. Hopkinson and K. W. M. Siu, *J. Phys. Chem. A*, 2000, **104**, 5023; G. Gilli and P. Gilli, *J. Mol. Struct.*, 2000, **552**, 1.

39 For reviews on the theoretical treatment of hydrogen bonding see: S. Scheiner, in *Reviews in Computational Chemistry*, eds. K. B. Lipkowitz and D. B. Boyd, VCH, New York, 1991, vol. 2, p. 165;

S. Scheiner, *Hydrogen Bonding: A Theoretical Perspective*, Oxford University Press, New York, 1997; J. E. Del Bene, in *The Encyclopedia of Computational Chemistry*, eds. P. v. R. Schleyer, N. L. Allinger, T. Clark, J. Gasteiger, P. A. Kollman, H. F. Schaefer III and P. R. Schreiner, John Wiley & Sons, Chichester, 1998, vol. 2, p. 1263.

40 T. Steiner and W. Saenger, *Acta Crystallogr., Sect. B*, 1994, **50**, 348.

41 G. Tóth, in *NMR Knowledge Base*, to be found under http://www.nmr.de/html/tricks/acidfree.htm, 1999.

42 V. Schepkin, T. Kawabata, H. J. Tritschler and L. Packer, *Free Radical Res.*, 1996, **25**, 195; J. V. Paukstelis, E. F. Byrne, T. P. O'Connor and T. E. Roche, *J. Org. Chem.*, 1977, **42**, 3941.

43 G. M. Sheldrick, SHELX-97, University of Göttingen, Germany, 1997.

44 DIAMOND, Visual Crystal Structure Information System, V. 2.1, Crystal Impact, Bonn, Germany, 1999.

45 C. Lee, W. Yang and R. G. Parr, *Phys. Rev. B*, 1988, **37**, 785; A. D. Becke, *J. Chem. Phys.*, 1993, **98**, 5648.

46 M. J. Frisch, M. Head-Gordon and J. A. Pople, *J. Chem. Phys.*, 1990, **141**, 189.

47 M. J. Frisch, G. W. Trucks, H. B. Schlegel, G. E. Scuseria, M. A. Robb, J. R. Cheeseman, V. G. Zakrzewski, J. A. Montgomery, R. E. Stratmann, J. C. Burant, S. Dapprich, J. M. Millam, A. D. Daniels, K. N. Kudin, M. C. Strain, O. Farkas, J. Tomasi, V. Barone, M. Cossi, R. Cammi, B. Mennucci, C. Pomelli, C. Adamo, S. Clifford, J. Ochterski, G. A. Petersson, P. Y. Ayala, Q. Cui, K. Morokuma, D. K. Malick, A. D. Rabuck, K. Raghavachari, J. B. Foresman, J. Cioslowski, J. V. Ortiz, B. B. Stefanov, G. Liu, A. Liashenko, P. Piskorz, I. Komaromi, R. Gomperts, R. L. Martin, D. J. Fox, T. Keith, M. A. Al-Laham, C. Y. Peng, A. Nanayakkara, C. Gonzalez, M. Challacombe, P. M. W. Gill, B. G. Johnson, W. Chen, M. W. Wong, J. L. Andres, M. Head-Gordon, E. S. Replogle and J. A. Pople, Gaussian 98, Rev. A.7, Gaussian, Inc., Pittsburgh PA, USA, 1998.